Received: 30 January 2016 | Revised: 27 February 2017 | Accepted: 5 July 2017

DOI: 10.1002/stc.2076

RESEARCH ARTICLE

WILEY

An improved equivalent force control algorithm for hybrid seismic testing of nonlinear systems

Zhen Wang[1,2,3] | Bin Wu[1,2,3] | Guoshan Xu[1,2,3] | Oreste S. Bursi[4]

[1]Key Lab of Structures Dynamic Behavior and Control of the Ministry of Education, Harbin Institute of Technology, Harbin 150090, China

[2]Key Lab of Prevention and Mitigation of Civil Engineering Disasters of the Ministry of Industry and Information Technology, Harbin Institute of Technology, Harbin 150090, China

[3]School of Civil Engineering, Harbin Institute of Technology, Harbin 150001, China

[4]Department of Civil, Environmental and Mechanical Engineering, University of Trento, Via Mesiano 77, Trento 38123, Italy

Correspondence
Zhen Wang, School of Civil Engineering, Harbin Institute of Technology, Harbin, 150090, China.
Email: zhenwang@hit.edu.cn

Funding information
National Key Research and Development Program of China, Grant/Award Number: 2016YFC0701106; National Natural Science Foundation of China, Grant/Award Number: 51408157, 51308159 and 51408080; Natural Science Foundation of Heilongjiang Province of China, Grant/Award Number: LC201423, QC2013C055; China Postdoctoral Science Foundation, Grant/Award Number: 2013M531046

Summary

The equivalent force control (*EFC*) algorithm is a hybrid seismic testing method based on both an implicit integration algorithm and force feedback control. As it performs the computation of the numerical substructure with a fixed sampling number and some evaluations are not necessary, the EFC method is believed to be time-consuming for seismic testing of nonlinear systems with complicated numerical substructure model. In order to tackle this problem, the EFC method with varying sampling number (*vEFC*) has been conceived. The analysis of the vEFC method has shown that 2 traditional pseudodynamic testing (PDT) variants on the basis of implicit time integration schemes and numerical iteration, that is, the *IPDT1* method and the *IPDT2* method, can be recovered from the vEFC method. Moreover, the advantages of the vEFC method, such as fast response rate and compensation for control errors and possible slippage, are demonstrated.

KEYWORDS

equivalent force control method, implicit integration algorithm, iteration, pseudodynamic testing, slippage, varying sampling number

1 | INTRODUCTION

1.1 | Background and motivation

Since it was proposed in early 1970s, the pseudodynamic testing (PDT) method has been studied and applied by worldwide researchers for the earthquake response evaluation of both components and structures.[1–5] On the basis of substructuring, the method is so powerful that even word-class facilities for earthquake engineering endowed with shaking tables try to build modular reaction walls, allowing for PDT or real-time substructure test (RST) possibly combining

shaking tables and actuators connected to walls.[6] As a new member of hybrid testing methods, RST adopts real-time loading instead of quasistatic loading in PDT.[7–9] Lately, PDT with numerical substructures (NSs) modeled using finite element software[10] and complicated physical substructure[11] tends to be performed. To perform this kind of complicated PDT, traditional methods should be examined and sometimes improved.

The PDT method heavily relies on the numerical solution of the system of equations of motion for the emulated structure using a step-by-step integration scheme. In detail, numerical integration schemes can be classified as implicit, linearly implicit, and explicit.[9,12] A key advantage of an implicit scheme is that it can be unconditionally stable, whereas most explicit schemes are conditionally stable.[5] Lately, linearly implicit and explicit methods, which are unconditionally stable, are proposed and applied to PDT. These methods often require specimen stiffness estimated prior to actual test; given the specimen damage in the following test, the real stiffness is often less than the initial one, resulting in dissipation introduced to the structure. Conversely, implicit algorithms do not require any exact stiffness estimation due to iteration. One concern regarding implicit algorithms for PDT is the potential undesirable loading–unloading hysteresis during the iteration process. A reduction factor is applied to the displacement increments in each iteration step to reduce the chance of displacement overshoot and potential undesirable hysteresis in the work of Shing et al.[13] In order to obtain reliable test results using implicit schemes in PDT, different iteration schemes have been proposed.[5,14,15] Meanwhile, alternative methods have been conceived and validated in this context; see, for instance, real-time pseudodynamic substructure testing using a substepping technique to avoid spurious oscillations of the specimen due to iterations[16] or the equivalent force control (EFC) method developed by Wu and coworkers.[17–19] As a result, implicit schemes are attractive candidates for PDT of multi-degree of freedom (MDoF) structures.

The EFC method is a versatile substructure testing algorithm due to its possible applications to standard PDT, RST, and even effective force testing.[17] Up to now, in order to verify the method and/or evaluate structural dynamic responses, many analyses and experiments have been carried out, including (a) the RST on a single-DoF (SDoF) system with a spring specimen[18]; (b) the RST on an offshore platform with a magnetorheological damper specimen[17]; (c) the PDT on both SDoF and MDoF structures endowed with a buckling-restrained brace specimen[19]; and (d) the substructuring PDT of a full-scale masonry structure.[20] Besides, the proportional-derivative control, the proportional-integral (PI) control, and sliding mode control methods have been employed in the EFC method.[21] Characterized by the solution to the nonlinear algebraic system of equations of motion based on force feedback control, this method opens a door for rich resources of feedback control algorithms to improve the solution process, resulting in, for example, a unidirectional convergence. Given the unconditional stability of implicit algorithms and convergence of the EFC method with proper control design, the EFC method is more suitable to test MDoF systems than are traditional methods.

Even though great progress has been made with the EFC algorithm, one shortcoming may limit its application in view of the development trend of PDT. As it is carried out as a pure control problem, the numerical part has to be evaluated at the control frequency. For complicated PDT, the NS probably simulated using a finite element model requires longer time to be evaluated. Therefore, the EFC algorithm has to be slowed down to evaluate the NS. Nowadays, the EFC method is always conducted with fixed evaluation (sampling) number for each integration step. In practice, the necessary evaluation number varies due to the state of the NS, which means less for linear state and more for nonlinear state. This entails that varying sampling number is more reasonable. From this analysis, one can see that the EFC method is more suitable for real-time hybrid testing; and it is, even possible but not effective, namely, time-consuming, for PDT with complicated NS models. To circumvent this problem, this paper conceives a new variant of the EFC method by intruding convergence criterion of numerical iteration, that is, the EFC method with varying sampling number (*vEFC*). Further analysis on this method shows its interesting features, such as faster convergence rate than iteration schemes, slippage compensation; then this new scheme is more suitable for PDT with complicated NS model, physical substructure (PS) compared with traditional methods.

1.2 | Scope

With the above-mentioned developments, in order to decrease that computational burden, we introduce to the EFC method a convergence criterion for iterations, forming the EFC method with varying sampling numbers, that is, the vEFC method. Further, we intend to show that the vEFC method can be reduced to the traditional implicit PDT with iteration schemes (*IPDT*) under some conditions, and that it can meet different requirements in terms of computational burden and test time duration. Moreover, we want to reveal the advantages of the vEFC method on some challenging

application such as seismic testing of systems with slippage. Due to these features, the vEFC method is viewed to be robust, which means that it can meet different requirements of different PDT.

Therefore, this paper is organized as follows. Section 2 recalls the α-method and main characteristics of the EFC method, whereas Section 3 introduces the IPDT methods based on iteration. The vEFC method is conceived in Section 4. Subsequently, the vEFC method is compared with the aforesaid iteration methods, and the fact that both iteration schemes are particular cases of the vEFC method under some specific conditions is shown. Then, in order to examine analytical results obtained in Section 5, numerical simulations are performed in Section 6. Finally, the PDT of a mild nonlinear steel specimen endowed with slippage is conducted and commented on in Section 7.

2 | THE α-METHOD AND THE EFC METHOD

2.1 | The implicit α-method

The α-method conceived by Hilber et al.[22] is a collocation-based algorithm, very well known and extensively used in both structural dynamics and PDT for its second-order accuracy and parametric dissipation for unwanted high-frequency components of the response. Hence, it is used also herein, and for notation simplicity, only scalar quantities are considered.

The time-discretized equation of motion and the relevant displacement and velocity approximations of the α-method can be expressed as

$$\begin{aligned} &M_{\mathrm{N}}a_{\mathrm{N},i+1} + (1+\alpha)C_{\mathrm{N}}v_{\mathrm{N},i+1} - \alpha C_{\mathrm{N}}v_{\mathrm{N},i} + (1+\alpha)R_{\mathrm{N}}\left(d_{\mathrm{N},i+1}\right) - \alpha R_{\mathrm{N}}\left(d_{\mathrm{N},i}\right) + \\ &(1+\alpha)R_{\mathrm{E},i+1} - \alpha R_{\mathrm{E},i} = (1+\alpha)F_{\mathrm{N},i+1} - \alpha F_{\mathrm{N},i}, \end{aligned} \tag{1}$$

$$d_{\mathrm{N},i+1} = d_{\mathrm{N},i} + \Delta t v_{\mathrm{N},i} + \Delta t^2\left[\left(\frac{1}{2} - \beta\right)a_{\mathrm{N},i} + \beta a_{\mathrm{N},i+1}\right], \tag{2}$$

$$v_{\mathrm{N},i+1} = v_{\mathrm{N},i} + \Delta t\left[(1-\gamma)a_{\mathrm{N},i} + \gamma a_{\mathrm{N},i+1}\right], \tag{3}$$

where M_{N} and C_{N} are the concentrated mass and damping coefficient of the NS that is numerically modeled; $d_{\mathrm{N},\,i}$, $v_{\mathrm{N},\,i}$, and $a_{\mathrm{N},\,i}$ are the nodal displacement, velocity, and acceleration at the ith time step; R_{N} and R_{E} are the restoring forces of the NS and physical substructure (PS), respectively; $F_{\mathrm{N},\,i\,+\,1}$ is the external force imposed on the structure; Δt is the integration time interval; and α, β, and γ are user-defined parameters that govern the algorithmic properties of the method. For the case $\alpha = 0$, $\beta = 0.25$, and $\gamma = 0.5$, the well-known constant average acceleration method, that is, the *trapezoidal rule*, is recovered. Substituting Equations 2 and 3 into Equation 1 leads to

$$K_{\mathrm{PD}}d_{\mathrm{N},i+1} + (1+\alpha)R_{\mathrm{N},i+1} + (1+\alpha)R_{\mathrm{E},i+1} = F_{\mathrm{EQ},i+1}, \tag{4}$$

where

$$F_{\mathrm{EQ},i+1} = (1+\alpha)F_{\mathrm{N},i+1} - \alpha F_{\mathrm{N},i} + K_{\mathrm{PD}}d_{\mathrm{N},i} + C_{\mathrm{PD}}v_{\mathrm{N},i} + M_{\mathrm{PD}}a_{\mathrm{N},i} + \alpha R_{\mathrm{N},i} + \alpha R_{\mathrm{E},i}, \tag{5}$$

$$K_{\mathrm{PD}} = \frac{M_{\mathrm{N}}}{\Delta t^2\beta} + \frac{(1+\alpha)\gamma C_{\mathrm{N}}}{\Delta t\beta}, \tag{6}$$

$$C_{\mathrm{PD}} = \frac{M_{\mathrm{N}}}{\Delta t\beta} + \frac{(1+\alpha)\gamma C_{\mathrm{N}}}{\beta} - C_{\mathrm{N}}, \tag{7}$$

$$M_{\mathrm{PD}} = \left(\frac{1}{2} - \beta\right)\frac{M_{\mathrm{N}}}{\beta} + (1+\alpha)\left(\frac{\gamma}{2\beta} - 1\right)\Delta t C_{\mathrm{N}}. \tag{8}$$

In order to advance the time from t_i to t_{i+1}, Equation 4, which is a nonlinear equation with respect to $d_{\mathrm{N},+1}$, needs to be solved using numerical iterations or other methods. It is worth mentioning that the performance of any iteration method plays an important role in the PDT of civil engineering structures, especially the ones characterized by nonlinear phenomena at the boundaries, for example, friction and slippage.

2.2 | The EFC method

The EFC method can be adopted to solve nonlinear Equation 4 through force feedback control instead of numerical iteration approaches. The block diagram of the EFC method is shown in Figure 1, in which $T_{\mathrm{c}}(s)$ and $T_{\mathrm{A}}(s)$ are the transfer functions of the Equivalent Force (EF) controller and the loading facility, respectively; $T_{\mathrm{ES}}(s)$ is the transfer function from the specimen displacement to the restoring force of the PS. $F(d)$ is a displacement error model to relate the specimen displacement to the actuator displacement. When the system tends to the steady state, the EF feedback that equals the left-hand side of Equation 4 is approximate to the EF command, entailing that the displacement of the PS satisfies Equation 4. However, both control errors and acquisition errors significantly affect the solution.[17] Thus in order to decrease error accumulation, the solution at $(i + 1)$th step is updated by substituting the measured restoring force of the PS into Equation 4.[17] From the viewpoint of control theory, when the EF feedback monotonically approaches to the command, the undesirable loading–unloading hysteresis can be eliminated, which means properly designed controller can circumvent this above-mentioned concern.

Displacement control is often chosen as loading mode in PDT. As the left-hand side of Equation 4 can be viewed as three elements in parallel, it is preferable to load the system in displacement control mode. However, force control[23,24] in seismic testing is under development and is a potential candidate for the EFC method in the future. In order to realize displacement control for the EFC method and keeping in mind that the control variable is a force, a force–displacement conversion factor, marked as C_{F} in Figure 1, has been established, through which a force quantity is converted to a displacement. The optimal C_{F} is the derivative of the left-hand side of Equation 4 with respect to displacement. As it is difficult to evaluate on line a reliable tangent stiffness operator of the PS and the tangent stiffness is often much smaller than the pseudodynamic stiffness K_{PD}, the following expression has been adopted:

$$C_{\mathrm{F}} = \frac{1}{(1+\alpha)K_{\mathrm{N0}} + K_{\mathrm{PD}} + (1+\alpha)K_{\mathrm{E0}}}, \tag{9}$$

where K_{N0} and K_{E0} represent the initial stiffness of the NS and PS, respectively. One should note that inaccurate initial stiffness of the NS and PS can be used in this formula, as it is in essence an iteration, which is different from the case in some explicit algorithms, where inaccurate stiffness may introduce dissipation to the system.

The objective of the EF controller is to compensate for the dynamics and nonlinearity of the system to ensure that the EF feedback can trace the command both rapidly and accurately in a stable way. When a proportional-derivative EF controller is utilized, the EF feedback is characterized by a steady-state error; in this case, a feedforward gain expressed as

$$K_{\mathrm{F}} = \frac{1 + K_{\mathrm{P}}}{K_{\mathrm{P}}} \tag{10}$$

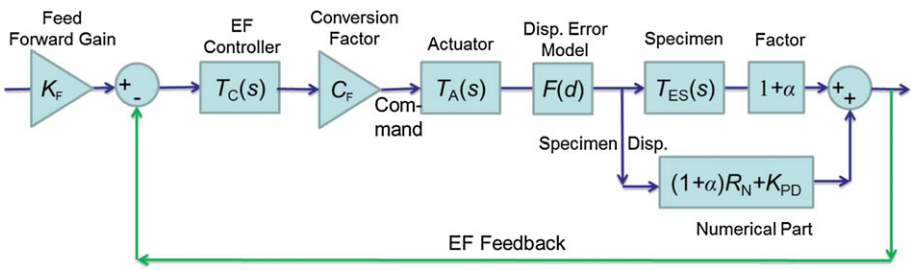

FIGURE 1 Block diagram of the equivalent force control method for a single-degree-of-freedom structure

can eliminate the relevant error inferred by Wu et al.[17] through a transfer function investigation for linear structures. Moreover, Wu et al.[18] pointed out that a PI EF controller can compensate for the steady-state error and then the feedforward gain K_F is not necessary. Lately, to avoid response overshooting and/or oscillation, Chen et al.[20] provided analytical expressions for suitable PI parameter ranges. Very recently, Wu et al.[21] resorted to employing a robust nonlinear sliding mode control in conjunction with the EFC method.

3 | THE α-METHOD VARIANTS DEVOTED TO PSEUDODYNAMIC TESTING

In practice, Equation 4 is often solved using numerical iteration methods, which result in IPDTs on the basis of a numerical iteration method. These methods were successfully conceived, validated, and applied in the past decades. In order to introduce a convergence criterion to the EFC method and analyze its performance, one of these methods is described herein.

Among numerical iteration methods, the Newton Downhill method exhibits favorable performance and is taken to solve Equation 4. Suppose

$$f\left(d_{\mathrm{N},i+1}\right) = K_{\mathrm{PD}} d_{\mathrm{N},i+1} + (1+\alpha) R_{\mathrm{N},i+1} + (1+\alpha) R_{\mathrm{E},i+1} - F_{\mathrm{EQ},i+1}. \tag{11}$$

The solution process with the Newton Downhill method to Equation 4 can be formulated as

$$d_{\mathrm{N},i+1}^{(k+1)} = d_{\mathrm{N},i+1}^{(k)} - \lambda \frac{f\left(d_{N,i+1}^{(k)}\right)}{f'\left(d_{N,i+1}^{(k)}\right)}, \tag{12}$$

where λ is the downhill factor used to enhance the smoothness of the convergence path, with $0 < \lambda \leq 1$; the superscript k represents the iterative step number. If $f'\left(d_{N,i+1}^{(k)}\right)$ is approximated by $(1+\alpha)K_{\mathrm{N0}} + K_{\mathrm{PD}} + (1+\alpha)K_{\mathrm{E0}}$, then one obtains

$$d_{\mathrm{N},i+1}^{(k+1)} = d_{\mathrm{N},i+1}^{(k)} - \lambda \frac{K_{\mathrm{PD}} d_{\mathrm{N},i+1}^{(k)} + (1+\alpha) R_{\mathrm{E},i+1}^{(k)} + (1+\alpha) R_{\mathrm{N}}\left(d_{\mathrm{N},i+1}^{(k)}\right) - F_{\mathrm{EQ},i+1}}{(1+\alpha)K_{\mathrm{N0}} + K_{\mathrm{PD}} + (1+\alpha)K_{\mathrm{E0}}}. \tag{13}$$

In PDT, the iterative displacement expressed by Equation 13 can be directly sent and imposed by the loading system to the PS, that is, $d_{\mathrm{C},i+1}^{(k+1)} = d_{\mathrm{N},i+1}^{(k+1)}$. However, the real displacement of the PS often differs from the command displacement due to control errors of the loading system, connector deformation, and slippage. In other words, the restoring force of the PS is related to the specimen displacement instead of the command displacement, that is, $R_{\mathrm{E},i+1}^{(k)} = R\left(d_{\mathrm{E},i+1}^{(k)}\right)$. Therefore, Equation 13 has to be expressed as

$$d_{\mathrm{N},i+1}^{(k+1)} = d_{\mathrm{N},i+1}^{(k)} - \lambda \frac{K_{\mathrm{PD}} d_{\mathrm{N},i+1}^{(k)} + (1+\alpha) R\left(d_{\mathrm{E},i+1}^{(k)}\right) + (1+\alpha) R_{\mathrm{N}}\left(d_{\mathrm{N},i+1}^{(k)}\right) - F_{\mathrm{EQ},i+1}}{(1+\alpha)K_{\mathrm{N0}} + K_{\mathrm{PD}} + (1+\alpha)K_{\mathrm{E0}}}. \tag{14}$$

As the terms on the right-hand side of Equation 14 are function of both $d_{\mathrm{N},i+1}^{(k)}$ and $d_{\mathrm{E},i+1}^{(k)}$, the resulting solution of Equation 14 may incorrectly converge or even diverge. Different remedies to this problem result in different methods for PDT using implicit algorithms. The most significant ones are treated herein.

3.1 | The IPDT1 variant

In order to circumvent the above-mentioned problem, a careful analyst can adopt

$$\begin{aligned} d_{\mathrm{C},i+1}^{(k+1)} &= d_{\mathrm{C},i+1}^{(k)} - \lambda \Delta d_{i+1}^{(k)} \\ \Delta d_{i+1}^{(k)} &= \frac{K_{\mathrm{PD}} d_{\mathrm{E},i+1}^{(k)} + (1+\alpha) R\left(d_{\mathrm{E},i+1}^{(k)}\right) + (1+\alpha) R_{\mathrm{N}}\left(d_{\mathrm{E},i+1}^{(k)}\right) - F_{\mathrm{EQ},i+1}}{(1+\alpha)K_{\mathrm{N0}} + K_{\mathrm{PD}} + (1+\alpha)K_{\mathrm{E0}}}, \end{aligned} \tag{15}$$

where the subscript C stands for "command." Clearly, the displacement $d_{\mathrm{N},i+1}^{(k)}$ in the second term of Equation 14 is replaced with $d_{\mathrm{E},i+1}^{(k)}$, resulting with $\Delta d_{i+1}^{(k)}$ only a function of $d_{\mathrm{E},i+1}^{(k)}$. This iteration scheme does not provide the solution to Equation 4 directly but the actuator command, which has the property of compensation for loading errors, as discussed herein. In fact, this method, called Variant 1—*IPDT1* variant—hereinafter, is the scheme adopted by Shing et al.[13] and results to be convergent for softening structures.[14] A convergence criterion is required to stop iterations; a standard displacement criterion reads as

$$\left|\Delta d_{i+1}^{(k)}\right| \leq \varepsilon, \tag{16}$$

where ε is a tolerance limit. Clearly, when Equation 16 is satisfied, the PS displacement is the convergent solution to Equation 4. In order to improve result accuracy due to the presence of sampling errors associated with the loading system, the structural displacement response and the specimen restoring force at the $(i + 1)$th step are finally corrected by

$$\begin{aligned} d_{\mathrm{N},i+1} &= d_{\mathrm{E},i+1}^{(n)} - \Delta d_{i+1}^{(n)} \\ R_{\mathrm{E},i+1} &= R\left(d_{\mathrm{E},i+1}^{(n)}\right) - K_{\mathrm{E0}} \Delta d_{i+1}^{(n)}, \end{aligned} \tag{17}$$

where n denotes the number of iterative steps. Then the acceleration and velocity responses can be updated according to the algorithmic assumptions. As a variant of numerical iteration, the command in Equation 15 should be effectively imposed on the specimen before the next iteration evaluation. In this way, the property of this iteration differs little from its pure numerical analysis. Otherwise, as the new command depends on the previous one and the previous specimen displacement, if the command is updated before the previous one is achieved or updated with an improper value of λ, the specimen displacement response may overshoot, leading to spurious hysteretic loops for a nonlinear specimen. Consequently, the iteration scheme has to be carried out with an updating period larger than the control settling time of the loading system; meanwhile, setting a proper value of λ is crucial. This feature leads to the lower loading rate of this method. One will find that the EFC method and the vEFC method can avoid this problem as both are to some extent based on control theory.

3.2 | The IPDT2 variant

An alternative method examined herein to determine the next command consists in using the specimen displacement instead of the command, namely,

$$\begin{aligned} d_{\mathrm{C},i+1}^{(k+1)} &= d_{\mathrm{E},i+1}^{(k)} - \lambda \Delta d_{i+1}^{(k)} \\ \Delta d_{i+1}^{(k)} &= \frac{K_{\mathrm{PD}} d_{\mathrm{E},i+1}^{(k)} + (1+\alpha) R\left(d_{\mathrm{E},i+1}^{(k)}\right) + (1+\alpha) R_{\mathrm{N}}\left(d_{\mathrm{E},i+1}^{(k)}\right) - F_{\mathrm{EQ},i+1}}{(1+\alpha) K_{\mathrm{N0}} + K_{\mathrm{PD}} + (1+\alpha) K_{\mathrm{E0}}}. \end{aligned} \tag{18}$$

This expression will be referred as Variant 2—*IPDT2* variant—hereinafter. Jung et al.[5] utilized a variant of this iteration method in fast hybrid simulation, where the PS displacement is different from actuator commands due to the actuator dynamics. In PDT, the difference can be caused by support slippage and elastic deformation of connectors.[25] Following Jung et al.,[5] the correction can be made by means of

$$\begin{aligned} d_{\mathrm{N},i+1} &= d_{\mathrm{C},i+1}^{(n)} \\ R_{\mathrm{E},i+1} &= R\left(d_{\mathrm{E},i+1}^{(n)}\right) - K_{\mathrm{E0}} \Delta d_{i+1}^{(n)}. \end{aligned} \tag{19}$$

One can find that Equation 18 provides the numerical solution to Equation 4; and thus, as it is only associated with the current specimen displacement, the actuator command can be updated at any instant, different from Variant 1. This method will not result in overshooting; however, an accurate result is not easy to obtain when error occurs between the command and the response of the specimen. Divergence of the iteration is one special case due to this error.

4 | THE EQUIVALENT FORCE CONTROL METHOD WITH VARYING SAMPLING NUMBER FOR PSEUDODYNAMIC TESTING

The above-mentioned EFC method has always been carried out with fixed sampling time and sampling number for each integration step. This entails that the time duration for each integration step is fixed as well. In practice, for the equivalent force feedback to approach the target, different sampling times are needed at different testing phases. Therefore, a varying sampling number is helpful in reducing the test time duration. Along this line, a convergence criterion can be introduced, leading to a new variant of the EFC method.

The block diagram of the improved version of the EFC method with varying sampling number, namely, the vEFC method, is depicted in Figure 2. In particular, "Next Step" represents the next integration step, whereas "Next Substep" means the next sampling step. Clearly, when $K_F = 1$, the output of the conversion factor block is identical to the second expression of Equation 15; hence, the stopping criterion 16 can be checked using this output. Therefore, once the conversion output is obtained, the convergence criterion is checked; if it is met, then update the displacement, velocity, and acceleration of this step and thus start up the next step; if it is not met, then evaluate the command output of the controller and then send to the loading system. The conversion factor block is moved ahead of the EF controller in this figure compared with Figure 1. For the case $K_F \neq 1$, Equation 16 is adopted as well to break the iteration.

5 | THE vEFC METHOD AND α-METHOD VARIANTS

In order to clearly reveal the performance of the vEFC method and to compare the vEFC method with the *IPDT* variants, this section concentrates on the solution process of Equation 4, which is the most important part of the *IPDT*. With a digital PI controller and a feedforward gain K_F, the actuator command reads as

$$d_{C,i+1}^{(k+1)} = C_F K_p \left(K_F F_{EQ,i+1}^{(k+1)} - F_{FB,i+1}^{(k)} \right) + C_F K_i \sum_{p=0}^{k} \left(K_F F_{EQ,i+1}^{(p+1)} - F_{FB,i+1}^{(p)} \right) \delta t, \tag{20}$$

in which δt is the sampling time; K_p and K_i denote the proportional gain and integral gain of PI control, respectively; $F_{EQ,i+1}^{(k)}$ and $F_{FB,i+1}^{(k)}$ represent the EF command and EF feedback at kth sampling instant of the $(i+1)$th time step. As the convergence criterion is adopted, the maximum value of $(k+1)$ varies for different integration steps. Note that a rectangular area instead of a trapezoidal one is used to approximate the integral of the PI control. In addition, the command at the previous sampling instant is

$$d_{C,i+1}^{(k)} = C_F K_p \left(K_F F_{EQ,i+1}^{(k)} - F_{FB,i+1}^{(k-1)} \right) + C_F K_i \sum_{p=0}^{k-1} \left(K_F F_{EQ,i+1}^{(p+1)} - F_{FB,i+1}^{(p)} \right) \delta t. \tag{21}$$

Subtracting the two equations above, one obtains

$$d_{C,i+1}^{(k+1)} = d_{C,i+1}^{(k)} + C_F K_p \left(K_F F_{EQ,i+1}^{(k+1)} - F_{FB,i+1}^{(k)} - K_F F_{EQ,i+1}^{(k)} + F_{FB,i+1}^{(k-1)} \right) + C_F K_i \left(K_F F_{EQ,i+1}^{(k+1)} - F_{FB,i+1}^{(k)} \right) \delta t. \tag{22}$$

As a result, we will see that, under specific conditions, the simplification of Equation 22 results in the IPDT1 variant and IPDT2 variant expressed by Equations 15 and 18, respectively.

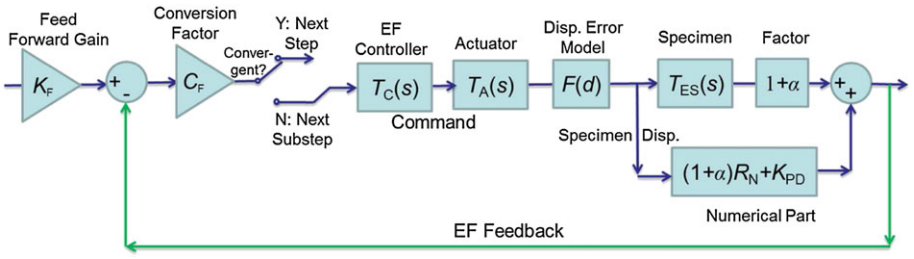

FIGURE 2 Block diagram of the vEFC method

5.1 | The vEFC method and the IPDT1 variant

When only the integral EF control is utilized in the vEFC method, denoted by the *I-vEFC* method, the displacement command of the actuator at the $(k+1)$th substep can be obtained by setting $K_F = 1$ and $K_P = 0$ in Equation 22, that is,

$$d_{C,i+1}^{k+1} = d_{C,i+1}^{k} + C_F K_i \left(F_{EQ,i+1}^{(k+1)} - F_{FB,i+1}^{(k)} \right) \delta t. \tag{23}$$

Provided that the EF command is sent as a step, that is, $F_{EQ,i+1}^{(k+1)} = F_{EQ,i+1}$, and that the block $\left[(1+\alpha) R'_{N,i+1} + K_{PD} \right]$ in Figure 2 is connected to the specimen displacement, one obtains

$$d_{C,i+1}^{k+1} = d_{C,i+1}^{k} - K_i \delta t \frac{K_{PD} d_{E,i+1}^{(k)} + (1+\alpha) R_N \left(d_{E,i+1}^{(k)} \right) + (1+\alpha) R_{E,i+1}^{(k)} - F_{EQ,i+1}}{(1+\alpha) K_{N0} + K_{PD} + (1+\alpha) K_{E0}}. \tag{24}$$

A careful reader can observe that Equation 24 is identical to Equation 15 if

$$\lambda = \delta t K_i. \tag{25}$$

For both the regular iterative steps and the first iterative step of each integration step, this conclusion is correct. As the same convergence criterion and correction can be adopted for both schemes, one can conclude that for a nonlinear equation, IPDT1 is identical to the I-vEFC method, a particular case of the vEFC method, when the EF command is sent as a step.

From the viewpoint of control theory, the vEFC method with a sophisticated control strategy, for instance PI control, can exhibit more favorable performance than with integral control, which is equivalent to the iteration scheme discussed above. One straightforward explanation is that searching space of the PI control contains the optimal value of the I control, which means that performance of PI control is not worse than that of I control. Therefore, for PDT with complicated NS model, the vEFC method can save time duration because the introduced convergence criterion and high-performance iteration scheme (i.e. the sophisticated control) can reduce the evaluation numbers of the NS model. Meanwhile, for PDT with demanding loading requirement, the vEFC method can update the loop with an interval greatly less than the settling time of the actuator and then saves time duration, as it is essentially a control problem. This differs from the case of the IPDT1 variant. As a result, the vEFC method can save time duration of IPDT compared with the IPDT1 variant. In fact, research revealed that stress relaxation due to long time duration leads to errors in PDT testing of RC components or structures.

5.2 | The vEFC method and the IPDT2 variant

When proportional EF control is utilized in the vEFC method, denoted by the *P-vEFC* method, the displacement command of the actuator at the $(k+1)$th substep can be attained in a similar way, resulting in

$$d_{C,i+1}^{(k+1)} = C_F K_P \left(K_F F_{EQ,i+1}^{(k+1)} - F_{FB,i+1}^{(k)} \right). \tag{26}$$

If the EF command in one integration time is a step, and the feedforward gain K_F is calculated by means of Equation 10, Equation 26 yields

$$d_{C,i+1}^{(k+1)} = \frac{(1+K_P) F_{EQ,i+1}}{(1+\alpha) K_{N0} + K_{PD} + (1+\alpha) K_{E0}} - \frac{K_P \left[K_{PD} d_{E,i+1}^{(k)} + (1+\alpha) R_N \left(d_{E,i+1}^{(k)} \right) + (1+\alpha) R_{E,i+1}^{(k)} \right]}{(1+\alpha) K_{N0} + K_{PD} + (1+\alpha) K_{E0}}. \tag{27}$$

Then for a linear structural problem, one gets

$$d_{C,i+1}^{(k+1)} = d_{E,i+1}^{(k)} - (1+K_P) \frac{K_{PD} d_{E,i+1}^{(k)} + (1+\alpha) R_N \left(d_{E,i+1}^{(k)} \right) + (1+\alpha) R_{E,i+1}^{(k)} - F_{EQ,i+1}}{(1+\alpha) K_{N0} + K_{PD} + (1+\alpha) K_{E0}}. \tag{28}$$

Hence, if $\lambda = 1 + K_P$, then the P-vEFC method for a linear structural problem is the same as IPDT2 expressed in Equation 18. Meanwhile, the same convergence criterion can be employed to both schemes. Accordingly, one can

deduce that IPDT2 is a particular case of the vEFC method for a linear structural problem. Note that for a nonlinear structural problem, as K_{PD} is often much greater than K_E and K_N, Equation 28 is often met in an approximate manner. With $0 < \lambda \leq 1$ in mind, one attains $-1 < K_P \leq 0$ using $\lambda = 1 + K_P$. Herein, a proportional control in conjunction with a feedforward gain K_F expressed by Equation 10 is applied, and therefore, a negative value of K_F is possible.

The drawbacks of the P-vEFC method occur to the IPDT2 method as well. One problem of the P-vEFC method is the steady-state error for a nonlinear loading system. The feedforward gain is proved to be effective for eliminating the steady-state error in the EFC method using proportional-derivative control.[17] However, for a nonlinear loading system, the steady-state error may not be eliminated by K_F alone. In fact, let us assume that there is a difference between the actuator command and the specimen displacement, that is,

$$d_{E,i+1}^{(k)} = \begin{cases} d_{C,i+1}^{(k)} - x_m & d_{C,i+1}^{(k)} \geq x_m \\ 0 & -x_m < d_{C,i+1}^{(k)} < x_m \\ d_{C,i+1}^{(k)} + x_m & d_{C,i+1}^{(k)} \leq -x_m \end{cases} \tag{29}$$

This entails that a constant slippage x_m exists between the specimen and its support. Evidently, if $d_{C,i+1}^{(k)} \geq x_m$ and $\lambda \Delta d_{i+1}^{(k)} = x_m$, the iteration cannot effectively update the displacement command. If the convergence tolerance $\varepsilon < \lambda^{-1} x_m$, then the iteration diverges and a displacement error of about $\lambda^{-1} x_m$ occurs to the specimen. Even though the correction procedure may enhance the accuracy of the solution to Equation 4, the real state of the specimen cannot be corrected.

This analysis shows that the vEFC method under specific conditions is equivalent to the numerical iteration schemes used in the IPDT2 variant. The problem, that is, the steady-state error of the P-vEFC method, occurs to the IPDT2 method, entailing potential divergence. From the analysis, one can conclude that in view of slippage compensation the vEFC method with a sophisticated control strategy, for example, PI control, can exhibit a more favorable performance than the IPDT2 variant can.

6 | NUMERICAL SIMULATIONS WITH SDoF AND 2DoF SYSTEMS

Step simulations and time history simulations are carried out herein to corroborate analytical results presented in previous sections. The step simulations are performed on an SDoF system, whereas the time history simulations are carried out on both the SDoF system and a two-DoF system, respectively.

The emulated SDoF system is shown in Figure 3. Structural parameters are defined as follows: M_N = 943 t, K_N = 10.19 kN/mm, C_N = 0.5922 kNs/mm, and K_{E0} = 50.95 kN/mm. The specimen follows a bilinear hysteretic force–displacement relation with the initial stiffness K_{E0}, the yielding displacement of 30 mm, and the strain-hardening ratio of 0.115. Therefore, the initial natural frequency and damping ratio of the system are 3/s and 0.05, respectively.

The two-DoF system is depicted in Figure 4. The values of the masses, stiffness, and the hysteretic parameters are identical to the counterpart of the SDoF system whereas viscous damping is not considered. This parameter definition results in the natural frequencies of 1.85/s and 4.85/s, respectively. The external force f_e = 10.102 kN is introduced to the at-rest structure to excite it in step simulations; the El Centro earthquake (NS, 1940) with a peak ground acceleration of 0.13 m/s^2 is considered in the time history simulation of the SDoF system and 6.84 m/s^2 of the two-DoF system simulations. The equation of motion of the structure is discretized by the α-method with Δt = 0.02 s and $\alpha = 0$.

In order to take into account the dynamics of the loading system, one second-order actuator model is adopted,[17] characterized by

$$T_A(s) = \frac{\omega_A^2 e^{-\tau s}}{s^2 + 2\zeta_A \omega_A s + \omega_A^2}, \tag{30}$$

where ζ_A and ω_A are equivalent damping ratio and equivalent circular frequency, respectively; τ is a pure delay of the actuator, whereas s is the Laplace variable. In a greater detail, the following parameters are assumed: ζ_A = 0.782, ω_A = 49.0149 rad/s, and $\tau = 0$. In simulations, the transfer function of the actuator is discretized using the zero-order hold discretization with the time interval of 0.001 s. In order to consider slippage, x_m = 0.2 or 0.5 mm is taken into account.

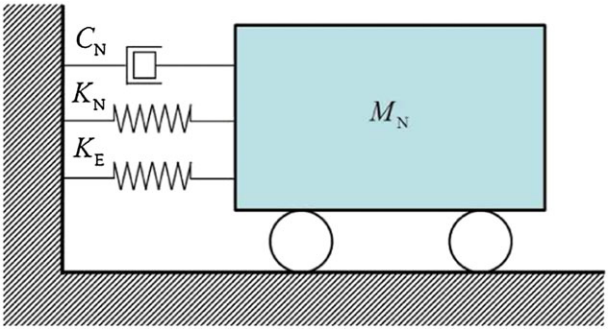

FIGURE 3 Schematic of the emulated single-degree-of-freedom system

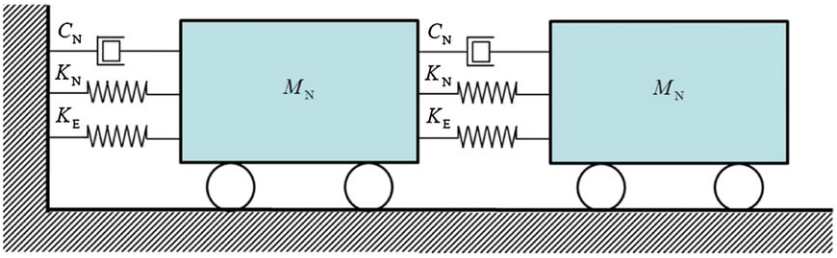

FIGURE 4 Schematic of the emulated two-degree-of-freedom system

6.1 | Step simulations for an SDoF system

Simulation results of IPDT1 combined with the vEFC method using different sets of parameters with or without slippage taken into account are shown in Figure 5. In the simulation, $\lambda = 0.3$ is adopted for IPDT1 and $K_i = \lambda/\delta t$ for the EF integral controller. For IPDT1, the parameter δt denotes the time period for iteration and command updating, whereas for the vEFC method, the sampling time for the EF loop. The results of IPDT1 with $\delta t = 0.2$ s are in good agreement with those of the I-vEFC method with the same sampling time in both cases. As $\delta t = 0.2$ s is greater than the settling time of the actuator model described in Equation 30, a series of step responses have been found. These simulation results verify the conclusions in Section 5.1 about the equivalence between the IPDT1 method and the I-vEFC method.

Simulation results of the vEFC method using PI control with $K_P = -0.2$ and $K_i = 1.5$ are provided in Figure 5 as well. This method is found to provide more rapid responses. The reason why the negative proportional gain can reduce the rising time is explained herein. At the beginning of this step, the EF feedback greatly differs from the EF command; hence the absolute value of the proportional term is large, and the command of PI control is small due to the negative proportional term. As both command and response are small, the integral term quickly accumulates error, and then the command increases faster than the does pure integral control. At some moment, the command of PI control catches up

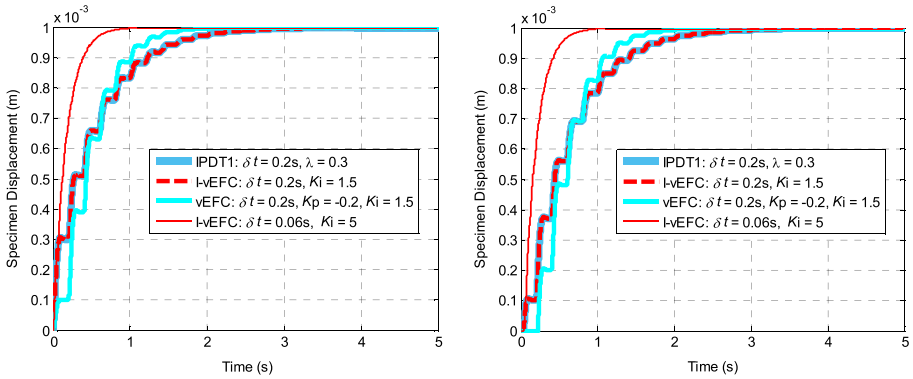

(a) Without slippage (b) With a slippage model of x_m=0.2 mm

FIGURE 5 Unit-step responses of the vEFC method combined with the IPDT1 method (a) without and (b) with slippage model of $x_m = 0.2$ mm

with that of I control, and then the former is larger than the latter. A larger command indicates a faster response and smaller rising time.

For the IPDT1 variant, the restoring force of the specimen is measured and fed back to the simulator after the displacement command has been imposed onto the specimen. In order to reduce the duration of the test with a simple NS model, the restoring force can be fed back at a faster rate for the vEFC method. Relevant simulation results with $\delta t = 0.06$ s are provided in Figure 5 too. One can observe that the duration is greatly reduced. The comparison between the vEFC method and the IPDT1 variant shows that PI control in conjunction with a smaller sampling time can improve the response speed. This fact entails that the total time consumed for the PDT using the vEFC method can be reduced, and therefore, the effect of stress relaxation on RC specimens due to too large test duration can be limited. With reference to slippage compensation, Figure 5 also shows the favorable performance of both methods, which is attributed to integral action. From this simulation, one can see that (a) for a test with complicated NS model, the vEFC method can reduce time duration by using sophisticated control compared with the IPDT1; and (b) for a test with simple NS model, the vEFC method can greatly reduce time duration by using smaller sampling interval compared with the IPDT1 method.

The comparison between the vEFC method with proportional control, that is, the P-vEFC method and the IPDT2 variant without and with slippage taken into account, is depicted in Figure 6. In the simulations, $\lambda = 0.3$ is adopted for the IPDT2 method and $K_p = \lambda - 1 = -0.7$ for the EF proportional gain. In the case of slippage, "Spec Disp" means the specimen displacement, whereas "Cmd" the displacement sent to the actuator as a command. Clearly, as shown in both cases, the two methods provide the same results whether the sampling time δt is greater or smaller than the settling time of the loading system with and without slippage. Differently from the case without slippage, in the case of slippage, the specimen displacements provided by both methods cannot converge to the target of 1 mm. The result provided by the I-vEFC method is plotted for comparison as well. Clearly, the specimen displacement approaches to the target by sending larger displacement command for the I-vEFC method.

The above-mentioned results validate the conclusions of Section 5.2: (a) the equivalence between the IPDT2 variant and the P-vEFC method for a linear structural system and (b) both methods may diverge when slippage is taken into account. These results entail that an outer displacement loop is necessary for the IPDT2 variant to compensate for slippage and other control errors. Hence, the vEFC method with sophisticated control, for example, PI control, is more suitable for hybrid seismic testing considering the error compensation.

6.2 | Time history analyses for an SDoF system

The comparison between the I-vEFC method and the IPDT1 variant is illustrated in Figure 7, where "Reference" denotes the simulation results of the whole structure evaluated using the constant average acceleration method with a time interval of 0.02 s. The same displacement convergence criterion (Equation 16) is applied to both methods with a tolerance limit of 0.01 mm. In order to stop the iterative loop for potential divergence, the maximum number of iterations was set to 50. Both the actuator model expressed by Equation 30 and the slippage model governed by Equation 29 with $x_m = 0.5$ mm are taken into account. The sampling interval 0.2 s is set given the numerical analysis of a complicated NS model, or complicated loading of the PS.

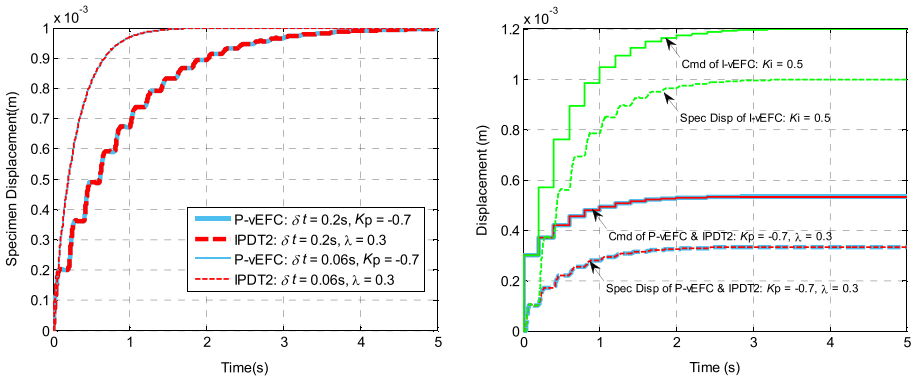

(a) Without slippage (b) With a slippage model of x_m=0.2 mm

FIGURE 6 Unit-step responses of the vEFC method combined with the IPDT2 method (a) without and (b) with slippage model of $x_m = 0.2$ mm

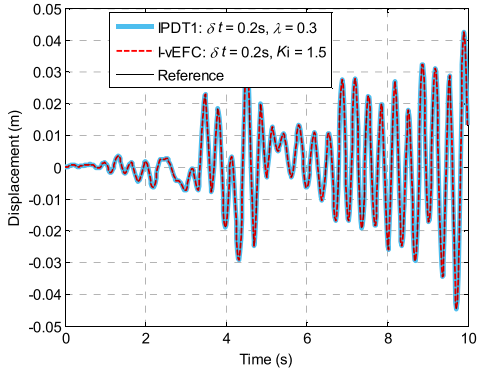

(a) Displacement time histories provided by different methods

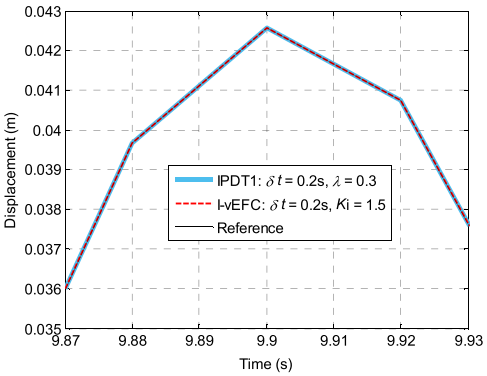

(b) Close-up view

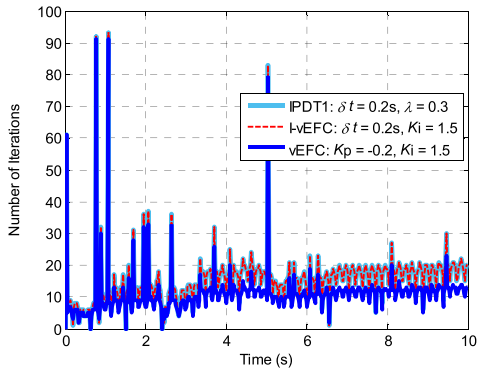

(c) Number of iterations for each step

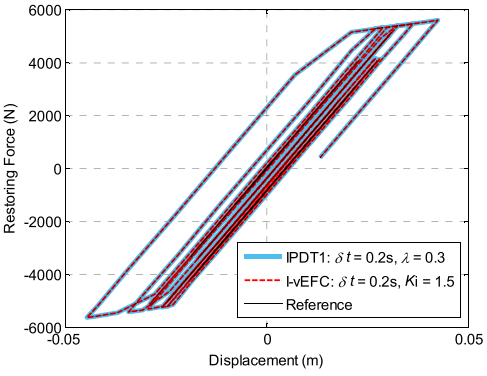

(d) Force-displacement relationships

FIGURE 7 Comparisons between the I-vEFC and the IPDT1 algorithm. (a) Displacement time histories provided by different methods, (b) close-up view, (c) number of iterations for each step, and (d) force–displacement relationships

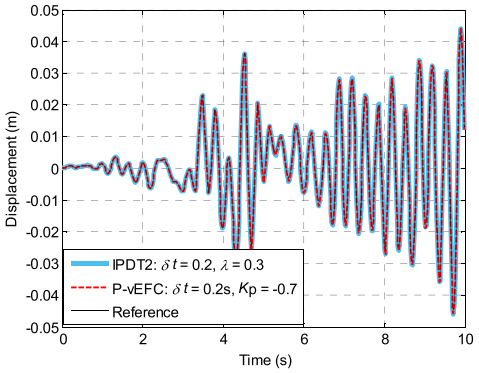

(a) Displacement time histories provided by different methods

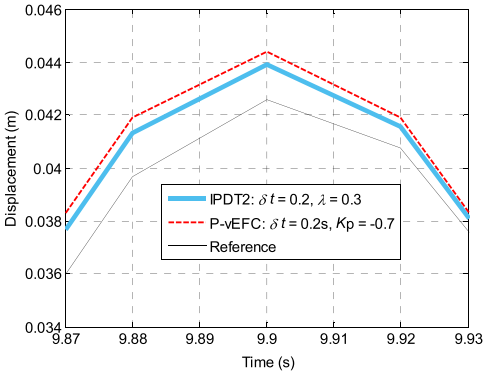

(b) Close-up view

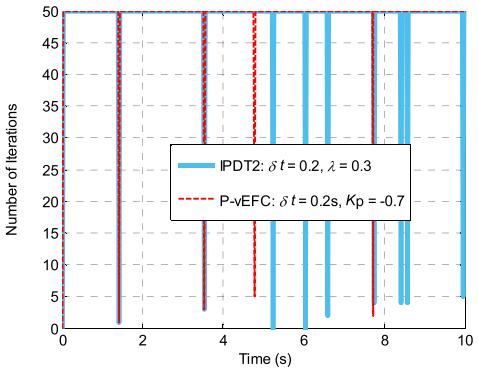

(c) Number of iterations for each step

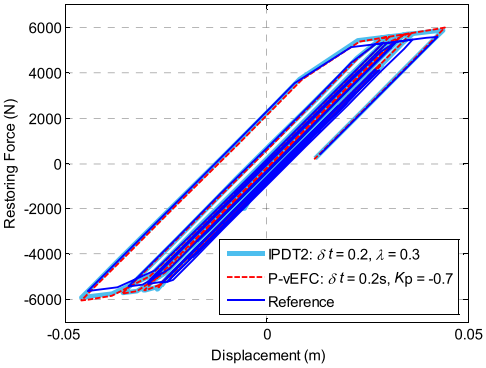

(d) Force-displacement relationship

FIGURE 8 Comparisons between the P-vEFC and the IPDT2 algorithm. (a) Displacement time histories provided by different methods, (b) close-up view, (c) number of iterations for each step, and (d) force–displacement relationship

Simulation results show that the I-vEFC method provides the same displacement response and force–displacement relation of the specimen with the same iteration number for each step. This verifies the conclusion that the IPDT1 variant is a particular case of the I-vEFC method. In order to examine its relevant advantages, the vEFC method with PI control is run with the number of iterations recorded and depicted in Figure 5(b). It is evident that the PI controller reduces the total number of iterations. In fact, the test duration is decreased by about one third due to the controller-based algorithm. This entails again that the vEFC method can save time duration by reducing the iteration amount with

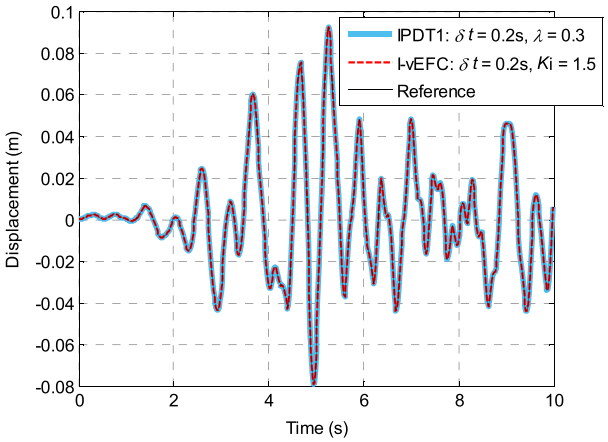

(a) Displacement time histories

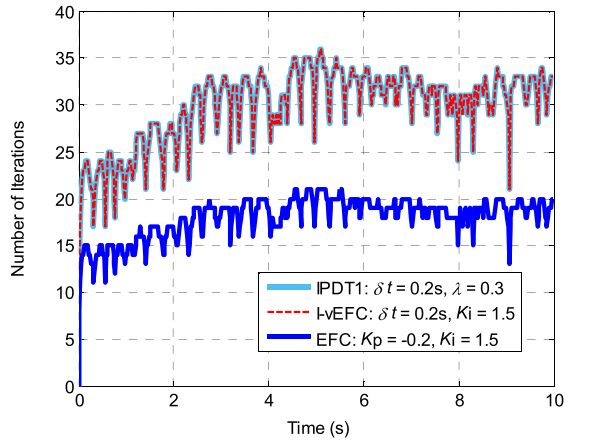

(b) Number of iterations for each step

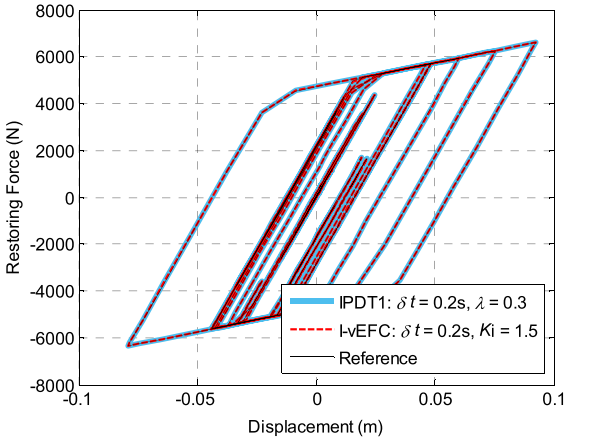

(c) Force-displacement relationships

FIGURE 9 Comparisons between the vEFC and the IPDT1 algorithm. (a) Displacement time histories, (b) number of iterations for each step, and (c) force–displacement relationships

the sophisticated control. As stated before, in view of the negative effect of stress relaxation, this reduction is quite meaningful for an improved accuracy. Furthermore, one can observe that the iteration number varies greatly; then, some evaluation steps of the EFC method with a fixed sampling number are not needed whereas some other steps may provide inaccurate solution. This analysis shows the necessity and advantage of the vEFC method proposed herein.

Simulations provided by the P-vEFC method and the IPDT2 variant are illustrated in Figure 8. In the first 4 s, the two methods provide the same results. This is attributed to the fact that the specimen exhibits a linear response in the first 4 s of simulation and that the P-vEFC method is identical to the IPDT2 method for a linear problem. When the specimen behaves in a nonlinear fashion, the constant factor used to eliminate the steady-state error cannot effectively work. Hence for most steps, the maximum iteration step is achieved entailing divergence, which is defined as the case that the convergence criterion is not met when iteration number rises to the maximum step. Figure 8(b) shows a close-up view of displacement comparison provided by different methods. Given the very good agreement in Figure 7(b), the differences herein are remarkable considering the strict convergence criterion. This simulation clearly shows that (a) for a linear structural problem, the IPDT2 is a particular case of the vEFC method, that is, the P-vEFC method; and (b) neither the IPDT2 nor the P-vEFC method can effectively compensate for specimen slippage.

6.3 | Time history analysis for a two-DoF system

In view of the shortcomings of the P-vEFC method, both the I-vEFC and PI-vEFC are further analyzed herein. For the sake of brevity, only responses relevant to the first storey of the two-DoF system are discussed herein, as depicted in Figure 9. In order to run simulations, the same parameters as those of Section 6.2 are employed whereas the same control parameters are employed for both stories.

From both displacement time histories and force–displacement relationships of the specimen, a reader can observe that the same conclusions drawn in Section 6.2 hold.

7 | VALIDATION TESTS

In order to further corroborate both analytical results and simulations, validation tests were carried out at the Mechanical and Structural Testing Center of the Harbin Institute of Technology. The schematic diagram of the overall emulated structure is shown in Figure 3 whereas the test setup in Figure 10. A steel column mounted onto the bottom beam with four bolts where main deformations and slip are localized was regarded as the PS. In order to monitor the absolute PS displacement, a Linear Variable Differential Transformer (LVDT) was installed as shown in Figure 10(b). In the tests, the NS was modeled and simulated by a dSpace DS1104 card; and the specimen was loaded by means of a Mechanical Testing & Simulation (MTS) system. In order to transfer data between the card and the loading system, data were first converted into analog signals, which were then resampled for the target system.

(a) Specimen and relevant actuator

(b) External LVDT used for measuring the top specimen displacement

FIGURE 10 Specimen and test setup. (a) Specimen and relevant actuator. (b) External LVDT used for measuring the top specimen displacement

The initial stiffness of the PS was found to be about 1.2×10^6 N/m, and the stiffness of the NS was chosen as $k_n = 1.5 \times 10^6$ N/m. The mass of the system was selected in such a way that the fundamental frequency of the overall elastic two-DoF structure was 1 Hz; in addition, the damping ratio of the structure was assumed to be 1%. In order to perform the tests, the vEFC method and the IPDT1 variant were employed with a time interval of 0.02 s. The IPDT1 variant was carried out with $\lambda = 0.3$ and $\delta t = 0.5$ s, the latter one set to obtain steady responses for each displacement command. The PI-vEFC method operated with $\delta t = 0.5$ s, $K_i = \lambda/\delta t$, and $K_P = -0.1$, whereas the I-vEFC method was used with $\delta t = 0.3$ s and $K_i = \lambda/\delta t$. For all tests, the convergence limit was set to 0.01 mm with a maximum iteration number equal to 11.

Test results are presented in Figure 11, where "D" means computational desired displacements. Moreover, note that the (test) time in the laboratory scale instead of the actual time is depicted in the x axis.

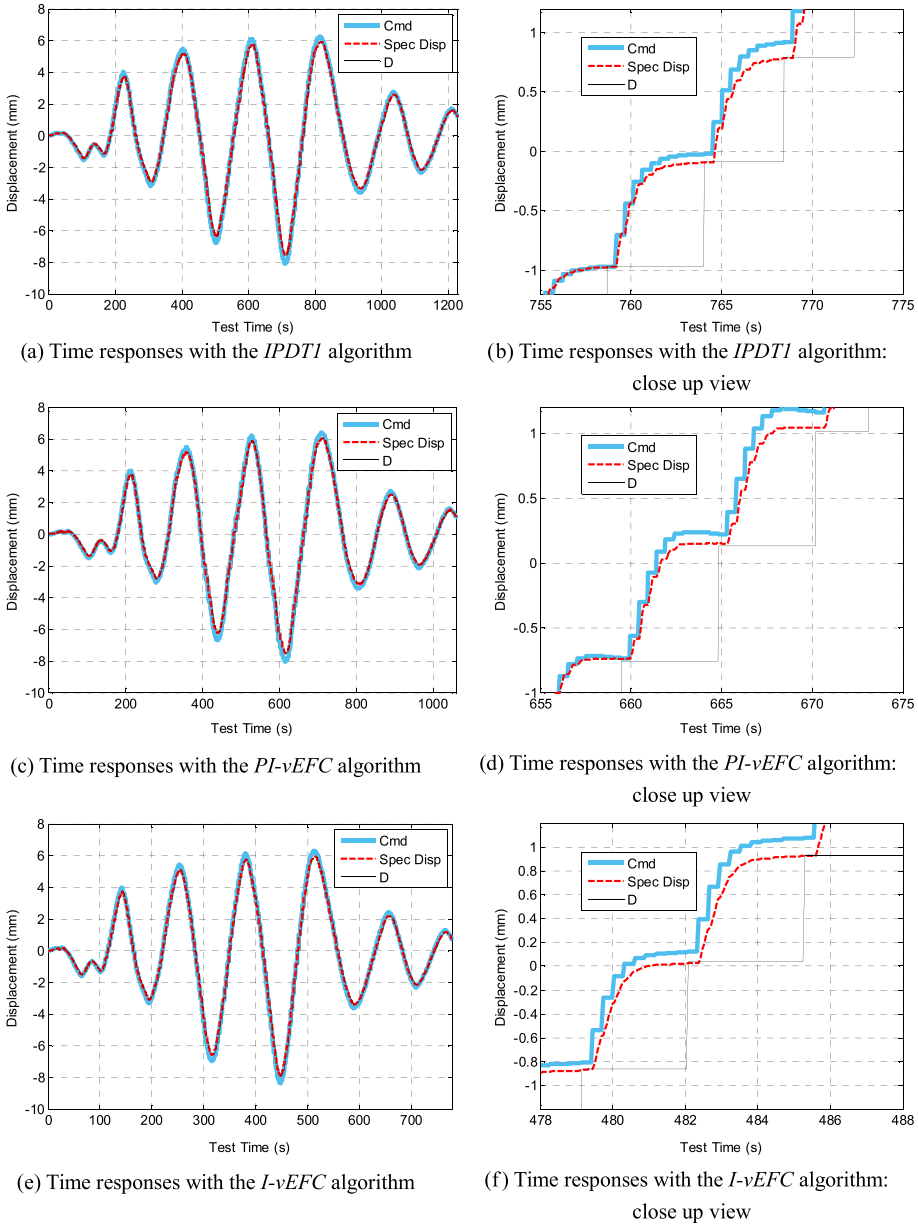

(a) Time responses with the *IPDT1* algorithm

(b) Time responses with the *IPDT1* algorithm: close up view

(c) Time responses with the *PI-vEFC* algorithm

(d) Time responses with the *PI-vEFC* algorithm: close up view

(e) Time responses with the *I-vEFC* algorithm

(f) Time responses with the *I-vEFC* algorithm: close up view

FIGURE 11 Displacement time histories and close-up views obtained with different algorithms. (a) Time responses with the IPDT1 algorithm. (b) Time responses with the IPDT1 algorithm: close-up view. (c) Time responses with the PI-vEFC algorithm. (d) Time responses with the PI-vEFC algorithm: close-up view. (e) Time responses with the I-vEFC algorithm. (f) Time responses with the I-vEFC algorithm: close-up view

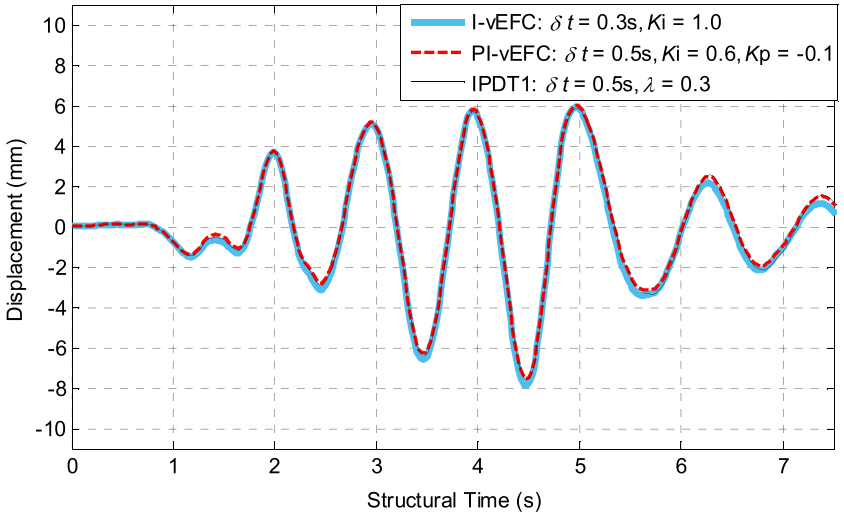

FIGURE 12 Comparison between desired displacements

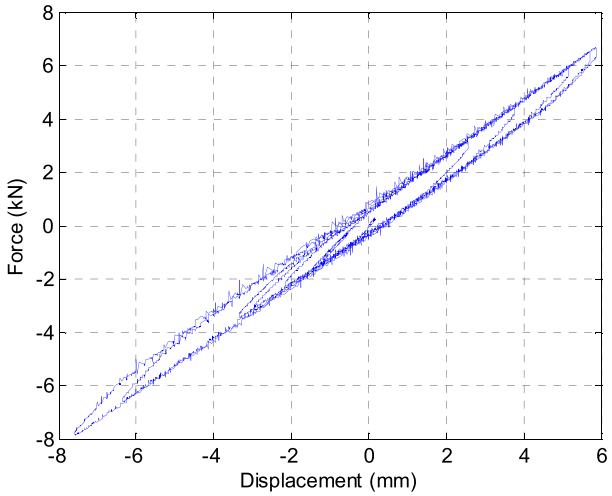

FIGURE 13 Displacement–restoring force relationship of the specimen

A reader can observe that the time duration of the three tests is about 1,220 s for the IPDT1 variant, 1,050 s for the PI-vEFC method, and 770 s for the I-vEFC method, respectively. This entails that, compared with the IPDT1 variant with the same δt, the PI-vEFC method successfully reduced the time duration by reducing sampling number and that the vEFC method with a faster updating speed can further reduce the duration than the IPDT1 method, even with the same parameter λ. These results are in agreement with analytical and numerical analysis presented in Section 5. For the case $\delta t = 0.5$ s, a series of step responses occurred to the specimen displacement response, whereas for $\delta t = 0.3$ s, the response was smoother. The commands of three tests were apparently different from the desired displacements and the specimen displacements, indicating the successfully compensated gap between the actuator and the specimen.

Desired displacement time histories computed in the above-mentioned three tests are depicted in Figure 12 for comparison, where the x axis denotes the actual structural time. From the figure, one can conclude that they closely match, despite the hysteresis of the specimen shown in Figure 13 and other uncertainties such as measurement noise.

8 | CONCLUSIONS

Lately, PDT tends to be performed with complicated NS model and physical specimen loading; to accomplish these tests, traditional methods should be examined and sometimes improved. In fact, the use of the EFC testing method to PDT

with complicated NS model is believed to be time-consuming, as it performs calculations of the NS with a fixed sampling number. In order to alleviate this problem, we have introduced a convergence criterion within iteration methods to the EFC method and conceived a new member of the EFC method, namely, the EFC method with varying sampling, that is, the vEFC method. The varying sampling number can reduce sampling number and hence save the test duration. In this respect, theoretical analyses and numerical simulations have shown that (a) the IPDT1 variant is identical to the vEFC method with integral control and stepped commands and (b) the IPDT2 variant for a linear structural problem is equal to the vEFC method with proportional control and stepped commands.

The advantages of the vEFC method endowed with a more sophisticated control, for example, the PI control, over both with the IPDT1 and IPDT2 methods have been analytically, numerically, and experimentally highlighted. In fact, with respect to the IPDT1 method, the vEFC algorithm can provide more rapid responses by tuning the controller parameters for PDT with complicated NS model and reducing the sampling interval for PDT with simple NS model, and hence save the time duration of PDT, leading to reduction of stress relaxation phenomena for components under testing. Moreover, the vEFC method can compensate for unwanted specimen slippage whereas the IPDT2 cannot and should be applied together with an outer displacement control. Therefore, in the case where the numerical computation is time-consuming, the vEFC method together with a larger sampling time does require the same or less computational burden as traditional methods, that is, the IPDT1 method. For other cases where the computation is fast and the loading performance is more demanding, the vEFC method with a more sophisticated control and a higher sampling frequency is endowed with better performance such as smaller time test duration. This feature entails that the vEFC method is surely more robust than are classical PDT methods.

This article proposed the vEFC method and validated its performance analytically, numerically, and experimentally. However, numerical and experimental simulations are simple but focused. Further investigations considering different excitations, NS model, specimens, and algorithmic parameters will be accomplished.

ACKNOWLEDGEMENTS

This research work is financially supported by the National Key Research and Development Program of China (grant 2016YFC0701106), National Natural Science Foundation of China (grants 51408157, 51308159, 51408080), China Postdoctoral Science Foundation (grant 2013M531046), and Natural Science Foundation of Heilongjiang Province of China (grants LC201423 and QC2013C055). The authors gratefully acknowledge their support. Nonetheless the conclusions are those of the authors and might not reflect the view of the sponsor agencies.

ORCID

Zhen Wang http://orcid.org/0000-0002-0859-4363
Bin Wu http://orcid.org/0000-0001-6768-533X

REFERENCES

[1] K. Takanashi, M. Nakashima, *J. Struct. Eng. ASCE* **1987**, *113*(7), 1014.

[2] S. A. Mahin, P. B. Shing, C. R. Thewalt, R. D. Hanson, *J. Struct. Eng. ASCE* **1989**, *115*(8), 2113.

[3] P. B. Shing, M. Nakashima, O. S. Bursi, *Earthq. Spectra* **1996**, *12*(1), 29.

[4] A. V. Pinto, P. Pegon, G. Magonette, G. Tsionis, *Earthq. Eng. Struct. Dyn.* **2004**, *33*, 1125.

[5] R. Y. Jung, P. B. Shing, E. Stauffer, B. Thoen, *Earthq. Eng. Struct. Dyn.* **2007**, *36*, 1785.

[6] F. Marazzi, I. Politopoulos, A. Pavese, *Bull. Earthq. Eng.* **2011**, *9*, 623.

[7] M. Nakashima, H. Kato, E. Takaoka, *Earthq. Eng. Struct. Dyn.* **1992**, *21*(1), 79.

[8] M. Ahmadizadeh, G. Mosqueda, A. M. Reinhorn, *Earthq. Eng. Struct. Dyn.* **2008**, *37*(1), 21.

[9] C. Chen, J. M. Ricles, T. M. Marullo, O. Mercan, *Earthq. Eng. Struct. Dyn.* **2009**, *38*(1), 23.

[10] T. Wang, M. Nakashima, P. Pan, *Earthq. Eng. Struct. Dyn.* **2006**, *35*(12), 1471.

[11] F. J. Molina, G. Verzeletti, G. Magonette, P. Buchet, M. Géradin, *Earthq. Eng. Struct. Dyn.* **1999**, *28*(12), 1541.

[12] O. S. Bursi, L. He, C. P. Lamarche, A. Bonelli, *J. Eng. Mech. ASCE* **2010**, *136*(11), 1380.

[13] P. B. Shing, M. T. Vannan, E. Carter, *Earthq. Eng. Struct. Dyn.* **1991a**, *20*, 551.

[14] P. B. Shing, M. T. Vannan, *Earthq. Eng. Struct. Dyn.* **1991b**, *20*, 809.

[15] A. Bonelli, O. S. Bursi, *Earthq. Eng. Struct. Dyn.* **2004**, *33*, 1067.

[16] V. Bayer, U. E. Dorka, U. Füllekrug, J. Gschwilm, *Aerosp. Sci. Technol.* **2005**, *9*(3), 223.

[17] B. Wu, Q. Wang, P. B. Shing, J. Ou, *Earthq. Eng. Struct. Dyn.* **2007**, *36*, 1127.

[18] B. Wu, G. Xu, P. B. Shing, *J. Earthq. Eng.* **2011**, *15*(1), 143.

[19] B. Wu, G. Xu, Y. Li, P. B. Shing, J. Ou, *J. Eng. Mech. ASCE* **2012**, *138*(11), 1303.

[20] Z. Chen, G. Xu, B. Wu, Y. Sun, H. Wang, F. Wang, *Earthq. Eng. Struct. Dyn.* **2014**, *43*(7), 969.

[21] B. Wu, H. Zhou, *Struct. Control Health Monit.* **2014**, *21*, 1284.

[22] H. Hilber, T. Hughes, R. Taylor, *Earthq. Eng. Struct. Dyn.* **1977**, *5*(3), 283.

[23] J. Zhao, C. Shield, C. French, T. Posbergh, *J. Struct. Eng.* **2005**, *131*(3), 244.

[24] N. Nakata, *Earthq. Eng. Struct. Dyn.* **2013**, *42*, 261.

[25] C. M. Chang, T. M. Frankie, B. F. Spencer Jr., D. A. Kuchma, *J. Earthq. Eng.* **2015**, *19*(2), 277.

How to cite this article: Wang Z, Wu B, Xu G, Bursi OS. An improved equivalent force control algorithm for hybrid seismic testing of nonlinear systems. *Struct Control Health Monit*. 2018;25:e2076. https://doi.org/10.1002/stc.2076